ELSEVIER

Journal of Chromatography A, 781 (1997) 161–183

JOURNAL OF CHROMATOGRAPHY A

Dynamics of capillary electrochromatography Experimental study on the electrosmotic flow and conductance in open and packed capillaries

Gargi Choudhary, Csaba Horváth*

Department of Chemical Engineering, Yale University, New Haven, CT 06520-8286, USA

Abstract

For capillary electrochromatography (CEC) to become an analytical separation technique of high speed and resolution the factors determining the conductivity of the column as well as the generation and control of electrosmotic flow (EOF) in porous media have to be understood. In the present study the conductance of capillaries packed with a variety of stationary phases was evaluated with respect to the conductance of the open capillary and the data were interpreted in the light of the Tobias equation. However, the consistently observed reduction of the EOF when a capillary having a charged inner wall is packed with particles having charges of the same sign and the dependence of the EOF velocity on the particle size needs further explanation. The data suggests that, due to the employment of relatively long columns packed with small particles, CEC may offer peak capacities much higher than HPLC or micro-HPLC. The CEC columns are unique as they consist of a packed and an open capillary segment having different conductances and consequently different voltage gradients and electrical field strengths. Therefore, any sufficiently detailed study on CEC systems requires also the characterization of the individual column segments. EOF velocities of 6–7 mm/s could be realized at 60 kV applied voltage with a 23/32 cm×50 μm raw fused-silica capillary packed with 6-μm Zorbax ODS particles. The current was a linear function of the field strength up to 1.8 kV/cm, but at high field strengths the EOF increased with squared field strength. Data on band spreading indicate that with a given column the plate height at high EOF velocities is smaller in CEC than in micro-HPLC and it is weakly dependent on the velocity. © 1997 Elsevier Science B.V.

Keywords: Electrochromatography; Electrosmotic flow; Capillary columns

1. Introduction

Capillary electrochromatography (CEC) is a branch of liquid chromatography employing packed capillary columns in high electric field with electrosmotic flow[1] of the mobile phase and electrophoretic migration of charged sample components. Thus, the key features of CEC are the generation of eluent flow by electrosmosis upon the application of high voltage and the separation of sample components due to differences in their distribution between the mobile and stationary phases and, if charged, in their electrophoretic mobilities as well. CEC is applicable to the analysis of both neutral and charged sample components and promises to offer much higher plate efficiencies than HPLC with packed capillaries (micro-HPLC). Furthermore, it is expected to offer higher loading capacity and a wider range of selectivity than CZE.

*Corresponding author.

[1]For the sake of brevity the words 'electrosmosis' and 'electrosmotic' suggested by von Smoluchowski [1] are used here.

0021-9673/97/$17.00
PII S0021-9673(97)00626-2

Since CEC shows many features common to micro-HPLC and CZE, it is most convenient to compare it to these two analytical separation techniques. On the other hand, upon comparing CEC to other differential migration processes of separation, which fall in the category of liquid chromatography, we may find the driving force of the mobile phase to be the most distinguishing characteristic. As seen in Table 1 only in micellar electrokinetic chromatography which employs a pseudo-stationary phase and in CEC is the flow of the mobile phase due to electrosmotic forces.

The practice of electrochromatography can be traced back to Mould and Synge [2,3] who used electrosmotic flow in the separation of polysaccharides on collodion membrane. In 1974, Pretorious et al. [4], suggested the use of EOF in both thin-layer chromatography and in column liquid chromatography with narrow bore packed columns. In 1981, Jorgenson and Lukacs [5] demonstrated the feasibility of CEC with packed glass capillaries. Tsuda [6,7] employed combined pressure driven flow and EOF in liquid chromatography with packed capillary columns.

Knox and Grant [8] showed that sufficient EOF can be obtained with eluent having ionic strength of 0.01 m and particles as small as 1.5 μm in diameter and separated aromatic hydrocarbons by CEC with plate efficiencies higher than those obtained in HPLC [9]. More recently, several groups have published their experimental work in capillary electrochromatography. Using 50-μm diameter capillaries packed with 3-μm diameter ODS Hypersil, Yamamoto et al. [10] obtained column efficiencies of 150 000–200 000 plates/m and reduced plate heights of 1.7–2.2. Yan et al. [11] used 320 μm I.D. fused-silica capillaries packed with 5-μm Spherisorb ODS for CEC and obtained reduced plate heights of 2–4. Smith and Evans [12] demonstrated reduced plate heights of 0.9–2 for columns packed with 3 and 1.5 μm alkyl-silica bonded phases and apparently of 0.04 for columns packed with 3-μm Spherisorb SCX [13]. They emphasized the need for pressurizing the buffer vials with inert gas to 500 p.s.i. in order to suppress bubble formation and avoid degassing the mobile phase at high currents, thus allowing the use of buffer concentrations higher than 10 m*M* (1 p.s.i.=6894.76 Pa). On the other hand, Boughtflower et al. [14] recommended the use of low conductivity buffers like Tris and 2-(N-morpholino)ethanesulfonic acid (MES) to reduce current and thus avoid pressurizing the buffer vials. Following a different approach, Behnke and Bayer [15] used an HPLC gradient pumping system to assist and enhance CEC separation by changing the solvent composition for gradient elution. Yan et al. [16] employed electrosmotically generated gradients for the elution of 16 polyaromatic hydrocarbons. Dittmann and Rozing [17] illustrated the effect of different organic modifiers on EOF and efficiency of separation in CEC.

The recent interest in CEC may stem from the possibility that it can be carried out with commercially available CZE instruments with minor alterations and from the increasing use of mass spectrometer as a detector with micro-HPLC and CZE. Thus, another MS-compatible high resolution analytical separation technique would expand the scope of multidimensional analysis of complex mixtures.

As the column is also the heart of CEC, the goal of this study is to examine the architecture of CEC columns and their operational features as well as to investigate experimentally some of the factors involved in the generation and control of EOF to point to the lacunae in our theoretical understanding of EOF field in porous media. The results are expected to facilitate the design of columns and operating conditions suitable for rapid separations with high efficiency in CEC.

Table 1
Driving forces for the mobile phase in various branches of liquid chromatography

Chromatographic method	Driving force
Classical and centrifugal liquid chromatography	Gravitational
Paper and thin-layer chromatography	Capillary
High-performance liquid chromatography	Hydraulic
Micellar electrokinetic and capillary electrochromatography	Electrosmotic

2. Theory

2.1. Effect of packing structure on conductance

The measurement of current in CZE and CEC serves as a diagnostic tool for certain properties of capillary columns and the chromatographic system at large [18]. Due to the distinctively different properties of packed and open capillaries, the situation in CEC is much more complicated than in CZE, that employs a simple open capillary tube. Whereas a great deal of experience has been accumulated with open capillaries in CZE [19,20], the properties of packed capillaries exposed to high electric field are yet to be explored.

In order to examine the change in conductance upon completely packing a given capillary tube with non-conductive particles, let's consider the following three hypothetical steps. First, the free cross-sectional area of the capillary column is reduced by the packing having an interstitial porosity, ε_e, so that the conductance of the column becomes $\kappa_o\varepsilon_e$, where κ_o is the conductance of the open capillary filled with the same electrolyte solution. Second, the conductance further decreases due to the tortuous and anfractuous packing structure that increases the effective migration length of the ions and reduces the electric field strength with respect to those of the open capillary. These effects are taken into account by the tortuosity factor, θ, so that the conductance of the packed capillary further decreases to $\kappa_o\varepsilon_e/\theta$, where θ is in the range from 1.5 to 3 [21]. Third, the cross sectional area of the channels, through which the ions migrate in the packed bed, is subject to dilation and contraction. Since, the decrease in field strength in the wider channels is not fully compensated for by the increased field strength in the narrower channels, this effect has to be corrected by the constrictive factor, χ [22]. Thus, in the absence of heat effects and other non-linearities, the conductance κ of the packed column is given by

$$\kappa = \frac{\kappa_o \varepsilon_e \chi}{\theta} \tag{1}$$

It follows from Eq. (1) that in CEC the ratio of the conductances of the packed and open forms of a capillary is given by the relationship

$$\frac{\kappa}{\kappa_o} = \frac{\varepsilon_e \chi}{\theta} \tag{2}$$

Parameters χ and θ are difficult to determine experimentally. Although there is an analytical expression for the dependence of χ on ε_e, it is rather complicated [22] even in its approximate version [23]. There is no relationship known between θ and ε_e although some authors [24] made the assumption that the tortuosity and the conductance ratio defined in Eq. (2) have the same dependence on the porosity.

In practice, an often cited relationship is Archie's law [25], which is based on empirical data obtained with rocks and other porous media and is given by

$$\frac{\kappa}{\kappa_o} = \varepsilon_e^m \tag{3}$$

where the exponent m ranges from 1.3 to 2.0. For spherical packing with $0.5 < \varepsilon_e < 0.7$ it is more appropriate to use the Tobias [26] equation

$$\frac{\kappa}{\kappa_o} = \varepsilon_e^{1.5} \tag{4}$$

which can be considered as a particular case of the simple power law given by Eq. (3).

The κ/κ_o ratio is expected, as long as the system is linear, to hold independently of the magnitude of EOF because EOF transports ions of both signs by convection at the same velocity and thus doesn't contribute to the current.

2.2. Electrosmotic flow in packed capillaries

The control of EOF is of great importance in CEC because the magnitude and reproducibility of the mobile phase velocity strongly affects the analytical results. So far the theoretical understanding of the electrosmotic flow field in packed columns is rather poor under the conditions employed in the practice of CEC. In the following, we briefly outline the well established theories for EOF in capillaries, which address the fundamental aspects of this type of flow, and define the EOF velocity frames of chromatographic interest.

2.2.1. Smoluchowskian model for EOF

The electrosmotic flow velocity, u_{EO}, of an elec-

trolyte solution along a flat charged surface under the influence of the electric field, V/L, is given by von Smoluchowski [27] as

$$u_{EO} = (\varepsilon_r \varepsilon_o \zeta V)/\eta L \quad (5)$$

where ε_o is the permittivity of vacuum, ζ the zeta potential of the surface, ε_r and η are the dielectric constant and the viscosity of the electrolyte solution, respectively. The assumption underlying Eq. (5) is that the double layer thickness is small compared to the characteristic length of the system. Despite its beguiling simplicity Eq. (5) has been found to express correctly the effect of viscosity, dielectric constant and zeta potential on the magnitude of the EOF velocity generated in capillary tubes [28] when the above assumption is met. For complex surfaces like those of the stationary phases employed in chromatography, however, the actual role of these parameters is still subject to a great uncertainty.

Rice and Whitehead [29] simulated trans-column flow profiles in a duct of cylindrical geometry by varying the ratio of the tube radius to the thickness of the double layer, r/δ. Assuming the absence of Joule heating, they found that when $r/\delta > 10$, the EOF profile is flat and independent of the tube radius. Indeed, several experimental studies in CZE [30] corroborated that barring Joule heating the tube diameter has no significant effect on the magnitude of EOF.

The applicability of Eq. (5) in CZE has given rise to modelling the column in CEC tacitly [8,31] as a bundle of capillaries [32] exhibiting Smoluchowskian EOF behavior. According to this approach the magnitude of EOF in packed columns would not be dependent on the particle diameter as long as the double layers do not overlap. This prompted Knox and Grant [8,9] to predict that the EOF flow velocity does not noticeably depend on the size of the particles as long as it is larger than 0.5 μm.

2.2.2. Velocity frames for EOF

The linear flow velocity of mobile phase through a packed CEC column is a significant operational parameter that affects the time of separation and the plate efficiency. In the following we provide a phenomenological description of the velocity frames of interest for the EOF.

In the engineering literature, the superficial flow velocity also called open tube flow velocity, is used for packed columns. It is defined in our case as the volumetric EOF rate F_{EO}, divided by the cross sectional area of the open column, A:

$$u_{EO,s} = \frac{F_{EO}}{A} \quad (6)$$

The interstitial velocity [33] of EOF, $u_{EO,e}$, is defined by

$$u_{EO,e} = \frac{u_{EO,s}}{\varepsilon_e} \quad (7)$$

where, ε_e is the interstitial porosity of the packed column which is given by the ratio of interstitial void volume and the empty tube volume.

In chromatographic practice an inert tracer is used for the measurement of the flow velocity of the eluent. In columns packed with porous particles the tracer explores both the interstitial and intraparticulate spaces and the velocity calculated from the column length and its hold up time is the so called chromatographic velocity [33]. When the eluent flow is electrosmotic, the chromatographic EOF velocity, $u_{EO,c}$, is given by

$$u_{EO,c} = \frac{u_{EO,s}}{\varepsilon_T} \quad (8)$$

In Eq. (8), ε_T is the total porosity of the column and its magnitude depends on the interstitial, ε_e, and the intraparticulate, ε_i, porosities as

$$\varepsilon_T = \varepsilon_e + \varepsilon_i(1 - \varepsilon_e) \quad (9)$$

For columns packed with nonporous particles $\varepsilon_i = 0$, thus, $\varepsilon_T = \varepsilon_e$, i.e., the total porosity equals the interstitial porosity so that the chromatographic EOF velocity measured with a neutral and uncharged tracer is the same as $u_{EO,e}$. Hence, the chromatographic EOF velocity in a column packed with nonporous particles ($\varepsilon_T = 0.4$) is higher than that obtained with the same capillary packed with porous particles of the same size and zeta potential under otherwise identical conditions.

2.2.3. Darcy's law and electrokinetic permeability

The relationship between the average flow velocity of an incompressible fluid and the pressure drop in a

packed bed is given by the linear phenomenological equation called Darcy's law [34] which can be written for the chromatographic flow velocity, u_c, as

$$u_c = B_{DL} \frac{\Delta P}{\Delta L} \quad (10)$$

where, B_{DL} is the Darcy's law chromatographic permeability of the column. It is related to the particle diameter, d_p, the viscosity of the liquid, η, and the interstitial, ε_e, and total porosity, ε_T, of the packing according to the Kozeny–Carman equation [34] and for the chromatographic velocity is given as

$$B_{DL} = \frac{1}{\eta} \frac{d_p^2 \varepsilon_e^3}{180(1-\varepsilon_e)^2 \varepsilon_T} \quad (11)$$

Comparison of Eqs. (10) and (11) shows that to maintain a given flow velocity the pressure drop has to increase with the inverse of particle diameter squared.

We may express the dependence of the chromatographic EOF velocity, u_{EO}, on the electric field strength, E, by the relationship

$$u_{EO,c} = B_{EK} \frac{\Delta V}{\Delta L} = B_{EK} E \quad (12)$$

Eq. (12) is analogous to Eq. (10) so that the coefficient, B_{EK}, can be viewed as the electrokinetic permeability. It depends, of course, on the structural parameters of the column packing, the zeta potential at the surface and the properties of the mobile phase such as the ionic composition, the viscosity and the dielectric constant.

According to Eqs. (10) and (12) the flow velocity is proportional to the driving force, $\Delta P/\Delta L$, for viscous flow and $\Delta V/\Delta L$ for EOF. In both cases the proportionality constants are the respective Darcy's law and electrokinetic permeabilities. The paucity of our knowledge about the EOF field in porous media precluded so far the development of a model to relate B_{EK} to the properties of the packed column in CEC. On the other hand B_{EK} is rather easy to measure since it is nothing else than the 'electrosmotic mobility' of a suitable inert, uncharged tracer in the packed capillary that is given by the slope of the linear EOF velocity versus overall electric field strength plot. B_{EK} is also referred to in the literature as 'electrosmotic flow coefficient'.

3. Experimental

3.1. Chemicals and materials

Analytical grade phosphoric acid, sodium hydroxide and HPLC grade acetonitrile (ACN) were supplied by Fisher (Pittsburgh, PA, USA) and sodium borate by Mallinckrodt (Paris, KT, USA). Potassium hydrogenphthalate (pH 4.01) and potassium phosphate (pH 7.00) buffer standards for calibration of the pH meter were obtained from J.T. Baker (Philipsburg, NJ, USA), whereas potassium chloride–hydrochloric acid (pH 2.00) and potassium carbonate (pH 10.00) standard buffers were obtained from Fisher and Brand-Nu Labs. (Meriden, CT, USA), respectively. Deionized water prepared using Nano-Pure purification system (Barnstead, Boston, MA, USA) was used throughout. Acrylamide was obtained from BioRad (Richmond, CA, USA) whereas benzyl alcohol, benzaldehyde, *o*-dichlorobenzene, *p*-toluic acid, cinnamic acid, *p*-terbutyl benzoic acid, napthalene, fluoranthene, biphenyl and terphenyl were purchased from ChemService (West Chester, PA, USA). Trp–Gly–Gly–Phe–Met and Trp–Met–Asp–Phe were obtained from Sigma (St. Louis, MO, USA).

Fused-silica capillaries 50, 75 and 180 μm I.D. and 375 μm O.D. with polyimide cladding were obtained from Quadrex (Woodbridge, CT, USA). Spherical 2 μm fused-silica beads and 2 μm pellicular ODS particles were obtained from Glycotech (Hamden, CT, USA). Zorbax ODS particles of 3.5-μm particle diameter and 80 Å mean pore diameter as well as 6-μm particle diameter and 80 Å and 300 Å mean pore diameter, were from Rockland Technologies (Newport, DE, USA). Highly crosslinked non-porous polystyrene–divinylbenzene (PS–DVB) microspheres of 2 μm and 5 μm diameter as well as capillaries with PS–DVB innerlining were prepared in our laboratory [35]. PS–DVB stands for highly crosslinked styrene–divinyl benzene copolymer which is prepared by Dr. Xian Huang in our laboratory and is used in this study for innerlining of fused-silica capillaries and in form of non-porous spheres for column packing. PLRP gigaporous (mean pore diameter of 1000 Å) highly crosslinked styrene–divinylbenzene particles having 5, 8, 20 μm diameter were gifts from Polymer Labs. (Shropshire,

UK). Gigaporous strong cation exchange particles (PLSCX) of 8-μm diameter were also gifts from Polymer Labs.

3.2. Instrumentation

3.2.1. Capillary electrochromatograph

3.2.1.1. Schematics of the capillary electrochromatograph

Schematics of the home built capillary electrochromatograph equipped with a 90 kV dual power supply and pressurizable vials at both the column inlet and outlet is shown in Fig. 1. The 90 kV dual power supply consists of a 0–60 kV (1) and a 0–30 kV (2) units both from Spellman (Plainview, NY, USA). The construction of commercial capillary electrophoresis units allows the use of applied voltage only up to 30 kV in order to avoid arcking and dielectric breakdown at higher voltages. This limitation has been overcome in our design so that when the anode is at +60 kV and the cathode is at −30 kV a voltage as high as 90 kV can be applied. The 30 kV power supply is bipolar, i.e., allows for a reversible polarity and the 60 kV power supply is unipolar and permits the application of a positive voltage only. Consequently, with a column having negatively charged chromatographic surface, the above arrangement allows the operation with a cathodic EOF at voltage drops up to 90 kV but with anodic EOF the applied voltage is limited to 30 kV. A Model 197A digital multimeter (3) from Keithley Instruments (Cleveland, OH, USA) was used for current acquisition.

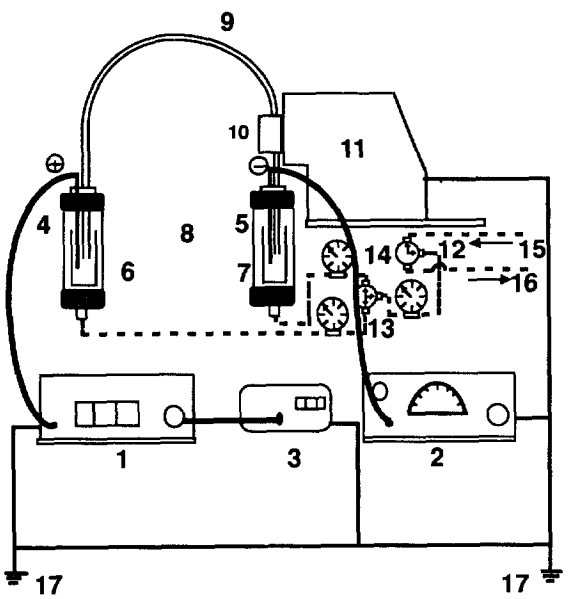

Fig. 1. Schematic of the modular capillary electrochromatograph with a 90 kV dual power supply and pressurizable chambers for the column inlet and outlet. (1) 60 kV power supply (2) 30 kV power supply (3) digital electrometer (4, 5) electrodes (6, 7) reservoir for mobile phase or the sample (8) pressurizable chambers (9) packed capillary column (10) cell for on-column detection (11) detector (12) four-port two-way valve (13) four-port three-way valves (14) pressure gauges (15) from nitrogen cylinder (16) vent (17) ground.

A Model SpectraFOCUS detector (11) and a Model 9550-0155 cell for on-column detection (10) both from Thermo Separation Products (Fremont, CA, USA) was used at 214 or 254 nm setting. In order to reduce the possibility of arcking, a 1.4-cm thick polyvinyl chloride (McMaster Carr, New Brunswick, NJ, USA) protective spacer block is mounted between the detector and the cell for on-column detection. A Model PS/2 77 486 personal computer (IBM, FL, USA) running OS/2 supported PC1000, version 3.0, data analysis software from Thermo Separation Products was used for data acquisition. In order to protect the column from breaking at the detection window a 17-cm long PTFE tubing, 0.050 cm I.D., 0.158 cm O.D., was installed between the bottom nut of the cell for on-column detection and the top of the pressurized reservoir to serve as a guide and sheath.

The vials (6, 7) containing 3 ml of the eluent, or the sample and housing the electrodes (4, 5) as well as the inlet and outlet ends of the column are kept in the two chambers (8) that are pressurizable up to 20 bar by nitrogen in order to suppress bubble formation in the column. The glass chambers with PTFE caps are 50 mm×17 mm I.D. chromatographic columns, Part Nos. 5710 and 5740 respectively, and were from Omnifit (Toms River, NJ, USA) with a Kel-F distributor for the pressurizing gas at the bottom. The PTFE caps of the chambers, were modified with a Delrin plug with two threaded ports for introducing and sealing in place with polyether ether ketone (PEEK) nuts the capillary and the electrode. The four-port three-way valve (13) facilitates pressurization of the buffer vials either individually or to-

gether. The four-port PTFE valves (12 and 13) from Omnifit are rated at 34 bar. Model WIK 2-400, 0–27 bar pressure gauges (14) were purchased from BOC Gases (North Haven, CT, USA).

3.2.1.2. Operation of the CEC unit

Prior to mounting the column in the CEC unit it is prequilibrated with the help of a high pressure pump at 400 bar for 30 min. The vials containing 3 ml of buffer are placed in the chambers. Thereafter, the prequilibrated column is mounted by first inserting the detection end of the capillary column through the cell for on-column detection and a guiding sleeve to reach the vial (7) that is placed at the end. While mounting, the detection window of the capillary column is aligned with the focusing lens of the on-column detection cell. Thereafter, the inlet end of the column is inserted into the vial (6) placed at that end. The mounting of the capillary has to be completed in a few seconds in order to avoid a drying of the capillary ends. The peak nuts are then tightened and the chambers containing the vials pressurized with nitrogen at 10 bar.

After mounting the packed capillary column is exposed to a voltage of 15 kV for 30 min before performing any runs during which the chambers containing the vials are pressurized simultaneously. The samples used in this study were injected electrokinetically for 2 s at 2 kV from the sample vial after both the chambers at the injection and the detection end were pressurized. For changing the eluent the column is removed from the electrochromatograph and equilibrated with the new eluent by using a high pressure metering pump.

3.2.1.3. Application of the voltage

When the surface of the capillary inner wall and the stationary phase carry negative charges a cathodic EOF can be generated. At applied voltages up to 30 kV the detection end of the column is kept at zero potential by turning power supply 2 on and keeping it at zero volt while power supply 1 is at voltages up to 30 kV. Alternatively, the injection end of the column can be kept at zero potential by turning the power supply 1 on and keeping it at zero volts while a voltage up to −30 kV is applied at the detection end. These two arrangements are equivalent. For voltages above 30 kV, only a cathodic EOF can be obtained. This is done by keeping the detection end at −30 kV and raising the voltage at the injection end to the desired value.

For cases where an anodic EOF is desired, which is the case when the chromatographic surface is positively charged, the polarity of power supply 2 is changed to positive, so that the detection end is now at +30 kV and the injection end is kept at zero volts. So far most experiments were conducted at applied voltages less than 30 kV.

3.2.2. CZE unit

All experiments with the open capillary columns were performed by using a P/ACE 2200 capillary electrophoresis unit (Beckman, Fullerton, CA, USA). In all experiments with the open capillary, the total capillary length and the corresponding migration distances were 27 and 20 cm respectively.

3.2.3. Packing device

A Milton Roy constaMetric III metering pump (Milton Roy, Riviera Beach, FL, USA) with stainless steel union present at the outlet end is used for testing the temporary retaining frit. An Altex Model 100A double reciprocating positive displacement pump (Beckman) with a maximum discharge pressure of 900 bar was used for packing capillary columns. The outlet from the pump is connected to a 50×2 mm I.D., stainless steel slurry reservoir with the help of 1 mm I.D., 0.158 cm O.D., stainless steel tubing.

3.3. Procedures

3.3.1. Column packing with siliceous particles

A slightly modified version of the packing procedure described by Boughtflower et al. [36] was adapted for the packing of siliceous particles into fused-silica capillaries having I.D. of 50–100 μm. Initially, a temporary retaining frit was prepared by sintering a 1–2 mm slug of 2 μm fused-silica beads (Glycotech) introduced at one end of the capillary column. Heat was applied from a high temperature flame generated with propane and oxygen by using a Type 3A blowpipe (Veriflo, Richmond, VA, USA). Subsequently, the frit was tested by applying 400 bar water pressure by the pump described above. Satisfactory frits produced a stable fine spray and let the

pressure relax to atmospheric in less than 5 s upon turning off the pump.

The column with the temporary retaining frit at the end is connected to a stainless steel slurry reservoir (50×2 mm I.D.) such that about 3 cm length of the column protrudes into the slurry reservoir containing the packing solvent and rinsed for 600 bar for 5 min. The capillary withstood this treatment without changes in the permeability of the frit.

With octadecylated silica particles, the slurry contained about 20 mg of solid in 220 μl of acetone–toluene (1:1, v/v). Reagent grade acetone was used as a packing solvent. With naked silica particles methanol–water (1:1, v/v) was used for the slurry and reagent grade methanol was the packing solvent. The slurry was sonicated for 10 min. Thereafter the slurry reservoir is filled with the appropriate slurry with the help of a syringe. Subsequently, 600 bar pressure was applied for ~1 h to compact and stabilize the packing. The pump was then turned off and the pressure allowed to relax slowly. The column was disconnected from the slurry reservoir, inspected under the microscope for uniformity of the packing and flushed with water at 400 bar for 30 min. In case of octadecylated silica the column is first washed with acetone, in order to remove residual toluene and then with water.

The final retaining frits are formed at the inlet and outlet end of the capillary column by sintering a 2-mm long slug of the stationary phase upon applying heat with a ring shaped heating element of 0.5-mm diameter while the column is being flushed with water at an inlet pressure of 400 bar. The heating element is made of 28 AWG Nichrom resistance wire (Omega, Stamford, CT, USA) and the temperature is controlled by a Variac. At the end, the temporary retaining frit was cut off and the excess packing was removed by reversing the flow direction.

3.3.2. Column packing with polymeric particles

PS–DVB or PLRP particles were packed in 180 μm I.D. capillaries. First a slug of wet 2 μm silica beads (Glycotech) was introduced at the column outlet with a tungsten wire, 150 μm in diameter, pushed about 10 cm into the capillary. Then the particles were sintered by applying heat with a Model 1000 microtorch (Microflame, Minneapolis, MN, USA). Subsequently, the capillary fitted with the frit connected to the bottom of the stainless steel slurry reservoir (40×4 mm I.D.) and washed with the packing solvent at an inlet pressure of 400 bar for 5 min. Acetonitrile–water (70:30, v/v) mixture was used as a packing solvent as well as the slurry solvent. The reservoir is filled with the slurry and the packing of polymeric particles at 400 bar took 2–5 min. The pump is turned off before reaching the desired packing length and the pressure was allowed to decline slowly so that the packing is not disturbed by a sudden release of pressure. During this process the height of the packing further increases. After reaching near atmospheric pressure the column is disconnected from the reservoir and washed at 400 bar pressure with the packing liquid for 60 min. The inlet end frit is prepared by placing a thin layer of 2-μm microspherical fused-silica particles (Glycotech) on the top of the PS–DVB beads which were then sintered by applying heat with the microring resistance heater as described above.

3.3.3. Measurement of operating parameters in CEC

The simplest and most common method for the measurement of the electrosmotic velocity is the use of an uncharged and unretained tracer although other methods of measurement have been reported in the literature. All measurements were at room temperature. In our experiments, acrylamide was used as a tracer for the measurement of the EOF velocity which was calculated by dividing the migration length, i.e., length from the inlet to the detection window by the time taken by the tracer to reach the detection point. The overall electric field strength is defined as the applied voltage divided by the total length of the column. In all experimental results we have reported the overall EOF velocity and the overall electric field strength.

3.4. Capillary columns

The capillary columns described here were made from raw fused-silica capillaries. However, for the investigation of the effect of the fixed charges at the capillary inner wall and the surface of the column packing on the magnitude of EOF, capillary columns

having unique properties were fabricated from 75 μm I.D. open fused-silica capillaries.

Open capillaries were lined with a fluid impervious thin PS–DVB inner tube the preparation of which is described elsewhere [35]. In one case, the PS–DVB inner surface was sulfonated and thus was negatively charged over the whole practical pH range. In the other case the inner tube was left unfunctionalized so that it did not have covalently fixed charges and was not expected to have a significant zeta potential.

For packing the capillaries having neutral and sulfonated PS–DVB inner tube, 2 μm monodisperse PS–DVB microsphere were prepared by polymerization method similar to that of making the PS–DVB inner tube. Columns were prepared by packing the capillaries having neutral or negatively charged inner wall by neutral or negatively charged microspheres. The unfunctionalized PS–DVB micro beads were not expected to have a significant zeta potential whereas the sulfonated PS–DVB had a strong negatively charges surface.

With these combinations we had two open tubular column, one with the neutral and the other with negatively charged inner wall. From these open tubes we obtain four different columns depending on the packing material. They are by the charge of the wall/charge at the packing surface: negative/negative, negative/neutral, neutral/negative, neutral/neutral. Greater details are found in Table 4.

4. Result and discussions

4.1. The dual make up of the columns in CEC

The equipment presently employed in CEC is patterned after the commercial CZE units featuring on-column detection. Downstream the packed capillary there is a segment of open capillary, that serves as connection to the vial containing the electrode and has a window for on-column detection. This is different from the situation in CZE where the entire capillary is open and the effect of the post-detection segment manifests itself mainly in a reduction of the effective voltage applied to the separating part of the column upstream the detection window.

In view of the present usage the column in CEC is

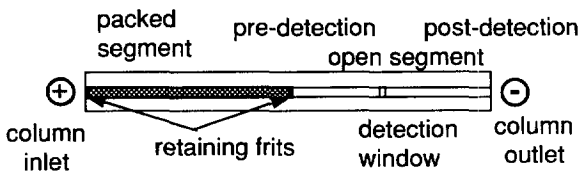

Fig. 2. Column architecture in CEC. The packed segment is followed by pre-detection and post-detection open tubular segments.

a complex construct and it can be divided, as illustrated in Fig. 2, into three parts: packed segment, pre-detection open segment and post-detection open segment. In the most frequently used configuration the detection point is located right after the frit. However, for the case shown in Fig. 2, where the detection point is located further downstream in the post-packing open segment, the sample components upon leaving the packed segment will migrate towards the electrode by convection due to EOF and those charged also by electrophoretic migration. Then band broadening is relatively modest particularly if the detection window is near to the end of the packed segment. The transition between the two segments and/or the not fully electrosmotic nature of the mobile phase flow in the open segment, however, can be the source of significant band spreading.

The duplex nature of CEC columns consisting of the packed segment of the capillary, i.e., the actual chromatographic column, followed by an open segment each having different conductances leads to different electric field strengths in the two segments as the current is conserved across the whole capillary tube. When the respective conductances of the packed and open segments are κ_p and κ_o then from Ohm's law and the conservation of the current it follows that

$$V_p\kappa_p = V_o\kappa_o = V_T\kappa_T \tag{13}$$

where V_p and V_o are the voltage drops across the packed (subscript p) and the open (subscript o) segments of the capillary, respectively. The respective electric field strengths, E_p and E_o, in the packed and open segments of the duplex CEC column can be calculated if the conductances and the lengths of the two segments as well as the corresponding voltage drops are know. Even though the current is the same in both the open and packed segments,

conditions for heat generation and transfer are likely to be different so that in CEC columns not only the electric field strengths but also the temperature fields in the packed and open segments can be expected to differ.

The mass conservation law requires the volumetric flow-rate of the liquid mobile phase to be the same in both the packed and open segments. Thus, the differences in the free cross sectional areas at the interface between the packed and the open segments of the capillary give rise to an abrupt decrease in the EOF velocity. Even if the capillary inner wall is charged, the EOF generated in the open segment will most likely not compensate for the effect of the increase in the free cross sectional area. If the capillary inner wall is uncharged there still can be a flow of the mobile phase upon degeneration of EOF to viscous flow. Thus, the flow field in the open segment will be affected not only by the entrance conditions and by the zeta potential at the capillary inner wall but also by the length of the different segments of the capillary. It follows from the foregoing discussion, that a precise evaluation of the pertinent column parameters in CEC requires attention to the axial changes in column properties.

4.1.1. Experimental study on the effect of column architecture

In order to demonstrate the effect of the packed and open capillary segments in duplex columns, we investigated the current versus voltage relationship with three raw fused-silica capillary columns: a 30 cm×50 μm open capillary without packed segment (column A), a 30 cm×50 μm duplex column with a packed segment of 10 cm (column B) and a 30 cm×50 μm duplex column with a packed segment of 20 cm (column C). In the fully open and the two duplex columns as well as in their open and packed segments the voltage drop, current, conductance, electric field strength and the rate of heat generation were evaluated and the data are presented in Table 2.

The results obtained with column A reflect the conditions in CZE since it is a fully open capillary column and therefore the values of the parameters

Table 2
The effect of partial packing of the capillary with the stationary phase on the various electric properties of the CEC system

		Column A $L_p = 0$ $L_o = 30$	Column B $L_p = 10$ $L_o = 20$	Column C $L_p = 20$ $L_o = 10$
		Total columns		
		$L_T = 30$ cm	$L_T = 30$ cm	$L_T = 30$ cm
V_T	(kV)	18	18	18
I	(μA)	6.6	3.9	2.6
κ_T	(μA/V)	0.36	0.21	0.14
E_T	(V/cm)	600	600	600
H_T	(mW)	119	70	46.8
		Packed segments		
		$L_p = 0$ cm	$L_p = 10$ cm	$L_p = 20$ cm
V_p	(kV)	NA	10.8	15.6
$\kappa_p L_p$	(μA cm/V)		0.0036	0.0032
E_p	(V/cm)		1080	780
H_p	(mW)		42	40.6
		Open segments		
		$L_o = 30$ cm	$L_o = 20$ cm	$L_o = 10$ cm
V_o	(kV)	18	7.2	2.4
$\kappa_o L_o$	(μA cm/V)	0.011	0.011	0.011
E_o	(V/cm)	600	360	240
H_o	(mW)	119	28	6.2

Column packing, 3.5 μm Zorbax ODS, 80 Å; mobile phase, ACN–10 m*M* borate, pH 8.0 (1:1, v/v).
The total capillary length, L_T, is 30 cm and the total applied voltage, V_T, is 18 kV.
The subscripts T, p and o stand for the total, packed and open segments of the capillary columns, respectively.

are the same throughout the column. Comparison of the data obtained with columns A, B and C shows that the total conductance, κ_T, is the highest with column A and lowest with column C, whereas in both columns B and C the conductance of the packed segment multiplied by their respective lengths, $\kappa_p L_p$, is about the same. The lower conductivity of packed capillaries in comparison to that of open capillaries facilitates the use of higher buffer concentrations and larger capillary diameters. Since the loading capacity of the column increases with the squared tube diameter, higher loading capacity can be obtained in capillary electrochromatography than in capillary zone electrophoresis [5].

Table 2 also provides a comparison of the rate of heat generation in the three columns. It is maximum in the fully open capillary column A, and minimal in column C. This is because at a given applied voltage the current in column A is much greater than the current in columns B or C. The rates of heat generation in the open and the packed segments in series of the duplex capillary columns are also listed in Table 2 and we see that in both columns B and C the rate of heat generation is significantly higher in the packed than in the open segments of these duplex capillary columns. This counterintuitive observation can be explained by the fact that the rate of heat generation, H, is inversely proportional to the conductance, i.e., $H=I^2/\kappa$, for a given current, I.

The data presented in Table 2 on the voltage and electric field strength in the three columns are illustrated in Fig. 3. It shows that across the entire length of column A the electric field strength is invariant whereas in both columns B and C there is an abrupt change in the field strength at the interface of the packed and open segments of the duplex columns. Despite such discontinuities in the present capillary electrochromatographic practice the effective values of the operational parameters are reported for duplex columns in toto. Therefore a caveat is necessary when using experimental data without sufficient details about the measurements.

4.2. Conductance in open and packed capillaries

In order to examine the applicability of Eq. (4) the conductances of open and partially packed raw fused-silica capillaries of the same inner diameter

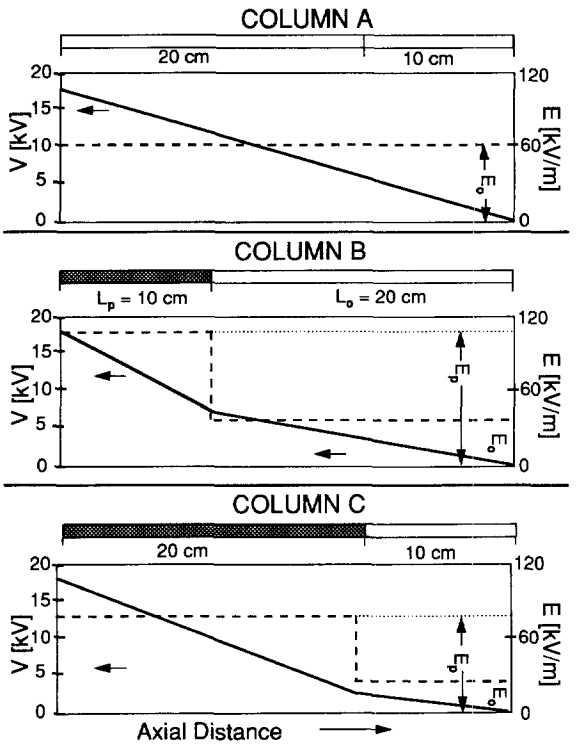

Fig. 3. Schematic illustration of the voltage drop, V, and electric field strength, E, across (a) a 30-cm long open capillary column (b) a CEC column with a packed segment of 10 cm and an open segment of 20 cm (c) a CEC column with a packed segment of 20 cm and an open segment of 10 cm.

were measured experimentally under otherwise identical conditions as far as the properties of the mobile phase and the capillary inner wall are concerned. The conductances of the open capillary, κ_o, and of the duplex capillary column, κ_T, were measured with a variety of packings believed to be non-conductive or to have significantly lower conductivity than the mobile phase. The conductance ratios, κ_T/κ_o, listed in Table 3 for the duplex capillary columns range from 0.38 for a 50-μm I.D. column packed with non-porous 2-μm HyTach silica microspheres to 0.5 for a 180-μm column packed with 20-μm gigaporous polymeric particles. The data show again that at the same applied voltage the electric field strength is lower in the duplex CEC capillary column than in the open capillary of the same length.

The ratio of conductance of the packed segment of

Table 3
Conductance ratios for capillary columns packed with various siliceous and polymeric support

Packing material	Particle size (μm)	Pore size (Å)	κ_T/κ_o	κ_p/κ_o
HyTach ODS	2	Non-porous	0.38	0.30
Zorbax ODS	3.5	80	0.4	0.35
Zorbax ODS	6	80	0.4	0.35
PS–DVB	2	Non-porous	0.4	0.33
PS–DVB	5	Non-porous	0.42	0.35
PLRP	5	1000	0.45	0.37
PLRP	8	1000	0.45	0.37
PLRP	20	1000	0.50	0.42

The column dimensions and the operating conditions are as in Figs. 4 and 6.

the duplex capillary to that of an open capillary of the same length and diameter, κ_p/κ_o, was also evaluated for all columns. Evidently, the κ_T/κ_o ratios are higher than the κ_p/κ_o ratios due to the duplexity of our CEC columns. Examination of the data in Table 3 also shows that columns packed with gigaporous particles have the highest conductance and those packed with non-porous particles the lowest. This is readily explained by the large interconnected pores of the gigaporous particles which allow ion transport across the particles. In any case the electric field strength is always reduced by the presence of packing and this is one of the reasons for the reduction of EOF upon packing a capillary tube.

In a rigorous analysis for the electrical conductivity of a porous plug with double layer much thinner than the radius of the particles O'Brien and Perrins [37] calculated a κ/κ_o value of 0.28 with a porosity of 0.4 and 0.44 with porosity of 0.6. The Tobias equation also gives a κ/κ_o ratio of 0.35 for porosity of 0.5. Thus, our experimentally obtained κ_p/κ_o values are in good agreement with κ/κ_o values predicted for $\varepsilon_e = 0.5$. The relatively high interstitial porosities observed with packed capillary columns are attributed to the small tube to particle diameter ratios as observed by Sternberg and Poulson [38] and with similar columns in gas chromatography [39].

4.3. EOF in columns packed with charged particles

In view of the great importance in CEC of the relationship between the particle size of the packing and the magnitude of the EOF, we investigated the effect of particle size on the electrosmotic flow velocity in columns packed with both porous and non-porous octadecylated silica particles and non-porous styrenic PS–DVB microspheres of different sizes. The results are shown in Fig. 4 by the plots of the EOF velocity versus overall field strength, i.e., the applied voltage divided by the total length of the duplex column. In all cases 50-μm I.D. raw fused-silica capillaries were employed and the EOF data are presented for both the open and packed capillaries as obtained at alkaline pH with a hydroorganic eluent.

It is seen that the EOF velocity in the open capillary is higher than that in any of the packed capillaries under otherwise identical operating conditions as far as the mobile phase composition and the tracer are concerned. This is in agreement with an earlier suggestion by Knox and Grant [9] that the electrosmotic velocity in a bed packed with impermeable spherical particles is smaller than that in an open tube having the same properties. As expected the EOF velocity in the column packed with 6-μm octadecylated silica particles is higher than in the column packed with unfunctionalized PS–DVB

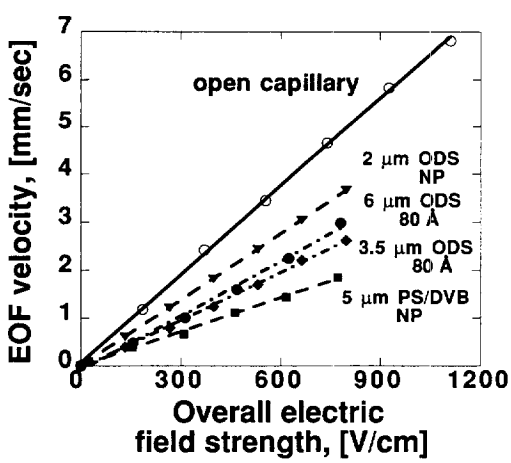

Fig. 4. Plots illustrating the dependence of overall electrosmotic flow velocity on the overall electric field strength. Columns, 20/27 cm×50 μm, open raw fused-silica capillary (thick solid line), 23/32 cm×50 μm, raw fused-silica capillaries packed with porous and non-porous octadecylated silica particles (dash dot lines) and with PS–DVB microspheres (thin dashed line); eluent, ACN–10 m*M* borate, pH 8.0 (4:1, v/v); tracer, acrylamide; injected for 2 s at 2 kV.

microspheres of the same size due to the higher zeta potential of the octadecylated silica particles that are negatively charged in contact with the alkaline mobile phase. The column packed with non-porous 2-μm ODS particles yielded the highest EOF velocity among the packed columns as expected in the light of the discussion in Section 2.2.2. This suggests that for rapid separation by CEC the use of micropellicular stationary phases [40,41] is advantageous.

From the data in Fig. 4 no conclusive information on the effect of particle diameter on EOF can be drawn. To a large part this is due to the fact that of the column packings were of different provenance and therefore their zeta potentials were likely to be different. The predictions based on the capillary bundle model with Smoluchowskian behavior notwithstanding, that the magnitude of EOF would not be dependent on the particle diameter, the data in Fig. 4 suggest a significant effect of the particle diameter on EOF. Expectations of EOF independent of particle size has been a strong inducement for the development of CEC [4] because in liquid chromatography with viscous flow the employment of long columns packed with very fine particles is precluded by the prohibitively high column inlet pressures required to generate sufficiently high flow velocities.

The data in Fig. 4 seems to indicate that the packing has a dual role as far as the magnitude of the EOF is concerned. The packing particles due to their charged surface facilitate the generation of EOF and at the same time serve as a drag for the flow. The interplay of these two effects determines the magnitude of the observed EOF. Further research is needed for the clarification of this issue and the results will likely show that there is an optimal particle diameter depending on the operating conditions in CEC.

Another way of looking at the role of the particle diameter and EOF relationship is offered in Fig. 5 which shows the relative magnitude of the electrokinetic and the Darcy's law permeability, vide Section 2.2.3, as a function of the particle size with the data presented in Fig. 4. The ratio of the permeabilities for the electrically and the pressure driven flow is the greatest with 2-μm particles in agreement with earlier suggestions. From this point of view, therefore, with columns packed with small particles, the use of electrosmotic rather than pressure driven flow of the mobile phase, is preferable [4,9].

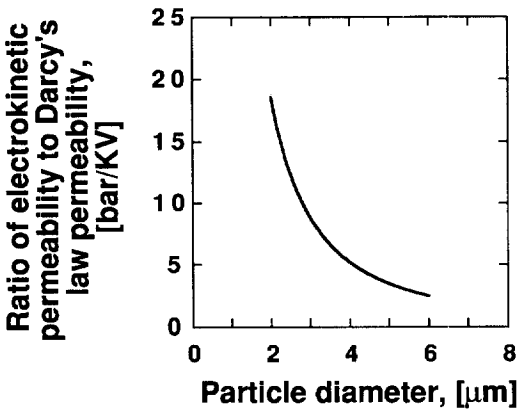

Fig. 5. Plot of the ratio of the electrosmotic permeability to viscous flow (Darcy's law) permeability, given by $\Delta P/\Delta V$, as a function of the particle diameter. The electrosmotic data were measured as follows: column, 23/32 cm×50 μm, raw fused-silica capillaries packed with octadecylated silica particles of different diameter; eluent, ACN–10 m*M* borate, pH 8.0 (4:1, v/v); tracer, acrylamide; injected for 2 s at 2 kV. The micro-HPLC data were obtained with the same columns and eluent described above.

4.4. EOF in columns packed with uncharged particles

Since Fig. 4 does not show a direct relationship between the particle size and the magnitude of EOF. In order to gain further insight into the effect of particle size, experiments were carried out by using four columns packed with highly cross-linked polystyrene particles in the range 2–20 μm. Theoretically, they are not supposed to have fixed charges at the surface and their zeta potential ought to be very small compared to that of the siliceous column packings, and for that matter to the inner wall of the fused-silica capillaries, at neutral or alkaline pH[2].

The results are illustrated in Fig. 6 by plots of the EOF velocity versus the overall electric field strength

[2] *Note added in proof.* We had recently an opportunity to measure the zeta potential of the unfunctionalized (PLRP) and the sulfonated PLSCX) 8 μm gigaporous styrenic particles suspended in ACN–water (1:1, v/v) with a Malvern instrument. The zeta potentials were −17.1 mV for PLRP and −33.9 mV for PLSCX.

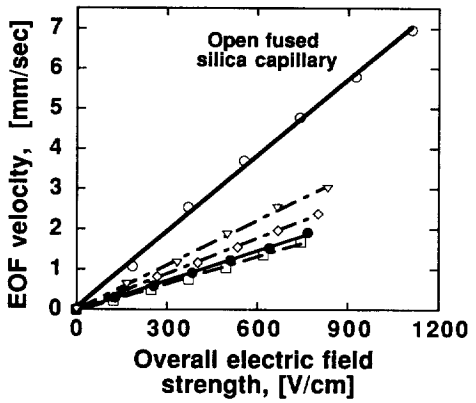

Fig. 6. Plots of the overall electrosmotic flow velocity against the overall electric field strength. Columns, 20/27 cm×180 μm, open raw fused-silica capillary and 30/40 cm×180 μm, raw fused-silica capillaries packed with (●) 2-μm, non-porous PS–DVB (□) 5-μm PLRP (◇) 8-μm PLRP and (▽) 20-μm spherical PLRP particles; eluent, ACN–10 m*M* borate, pH 8.0 (4:1, v/v); tracer, acrylamide; injected for 2 s at 2 kV. All PLRP particles have a mean pore diameter of 1000 Å.

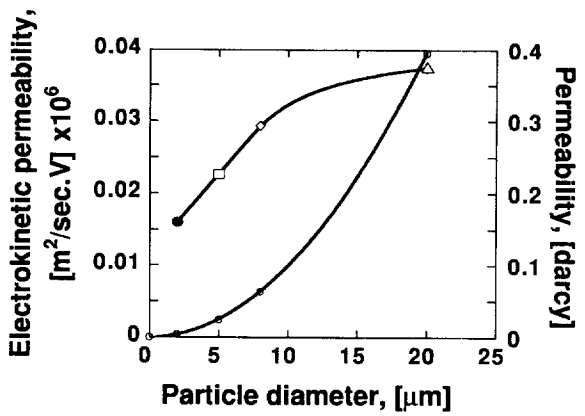

Fig. 7. Plots of the electrokinetic permeability and the Darcy's law permeability of raw fused-silica capillary columns packed with unfunctionalized spherical styrenic particles against the particle diameter. Columns, 30/40 cm×180 μm, packed with (●) 2-μm, non-porous PS–DVB, (□) 5-μm PLRP, (◇) 8-μm PLRP and (▽) 20-μm PLRP particles; eluent, ACN–10 m*M* borate, pH 8.0 (4:1, v/v); tracer, acrylamide; injected for 2 s at 2 kV. All PLRP particles have a mean pore diameter of 1000 Å. For consistency the data measured with the non-porous column packing was recalculated by assuming $\varepsilon_T = 0.6$ to obtain the equivalent chromatographic EOF velocity. The electrokinetic permeability of the open raw fused-silica capillary with the same eluent is $0.062 \cdot 10^{-6}$ (m^2/V s) from the data in Fig. 6.

with data obtained by using 180-μm I.D. raw fused-silica capillaries packed with particles of four different sizes and the same capillary without packing. In each case the EOF velocity and the current (not shown) is a linear function of the overall electric field strength and in each packed capillary column the EOF velocity is lower than that in the open raw fused-silica capillary of the same inner diameter at pH 8.0. It is seen that at a given applied voltage the EOF velocity increases with the particle diameter and the column packed with 20-μm PS–DVB particles exhibit the highest EOF velocity. The EOF velocity obtained with the non-porous 2-μm particles is higher than that with the 5-μm porous particles. This is due to the relatively greater mobile phase space (total porosity) of the column packed with porous particles as discussed above.

However, the relatively high EOF in columns packed with unfunctionalized styrenic particles may be due in part to the retaining frits which are made of silica.

For comparison the dependence of electrokinetic and Darcy's law permeabilities on the particle size is illustrated in Fig. 7. The electrokinetic permeability measured under the experimental conditions stated is a much weaker function of particle diameter than the Darcy's law permeability which increases with the squared particle diameter. In order to facilitate comparison the electrokinetic permeability of the column packed with the non-porous 2-μm particles in Fig. 7 was corrected to account for the lack of the intraparticulate pore volume.

Fig. 8 illustrates the lack of correlation between

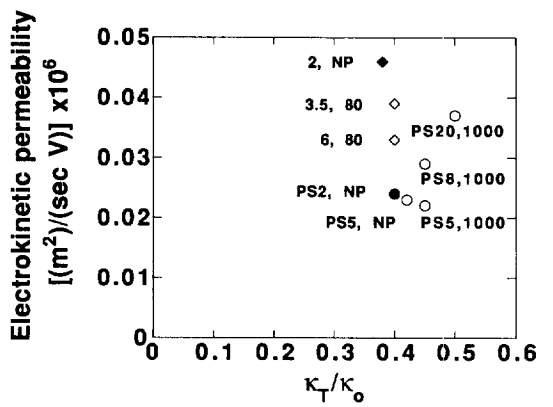

Fig. 8. Plot of electrokinetic permeability versus κ_T/κ_o. Columns, listed in Table 3; eluent, ACN–10 m*M* borate, pH 8.0 (4:1, v/v); tracer, acrylamide; injected for 2 s at 2 kV.

the electrokinetic permeability as measured by the mobility of acrylamide and the κ_T/κ_o ratio in the packed capillary columns employed in this study. The graph proves that the electrokinetic permeabilities of the columns are independent of the κ_T/κ_o ratio as discussed before. In essence, the permeability depends on the zeta potential of the particles whereas the conductance ratio is independent of the zeta potential as long as the double layer thickness is smaller than a tenth of the particle diameter as suggested in the literature [37].

4.5. Zeta potential of the capillary wall and the packing

Generally, the capillary inner wall and the surface of the stationary phase particles have fixed charges in CEC and the double layer formed at the surface in contact with the mobile phase accounts for the generation of EOF upon applying high electric field. In most practical applications of CEC, the charges at the tube inner wall and the surface of the column packing have the same sign to maximize the magnitude of EOF. For instance, with the use of raw fused-silica capillaries packed with octadecylated silica particles in capillary reversed-phase electrochromatography, both the inner wall of the capillary and the stationary phase surface have negative charges when the mobile phase has neutral or alkaline pH. In the following we describe a set of experiments aimed at the investigation of the effect of the charged or uncharged capillary wall or column packing on the magnitude of EOF. The columns used in these experiments are listed in Table 4 and were described in Section 3.4. All six columns were constructed so that their full lengths were lined with the fluid impervious inner tube and only in about 3-mm long detection window, placed right after the retaining frit at the outlet of the packed section was the bare fused-silica tube in contact with the mobile phase. As described in the experimental part, the two retaining frits were made by sintering silica particles. The experimental results shown below represent directly measured data without correction for the EOF due to these siliceous surfaces or the effect of the post-detection open segments of the column.

Table 4
Set of columns prepared for the study of the effect of the changes at the capillary innerwall and the surface of the packing[a]

Column	Innerwall	Packing	Electrokinetic permeability[b]
A	PS-SO_3^-	NA	0.063
B	PS	NA	0.020
C	PS-SO_3^-	PS	0.024
D	PS-SO_3^-	PS-SO_3^-	0.041
E	PS	PS	0.0056
F	PS	PS-SO_3^-	0.014

[a] The preparation of columns is described in Section 3.4.
[b] Slopes of plots of EOF against the overall electric field strength.

The EOF velocity was measured with columns A–F by using aqueous ACN–10 m*M* borate buffer, pH 8.0 (4:1, v/v) and with acrylamide as the tracer. Fig. 9 shows the plots of EOF velocity versus overall electric field strength. The data obtained with open capillaries, having either negatively charged (column A) or neutral inner wall (column B), are shown in Fig. 9a. As expected, the EOF velocity was much higher in column A, which had a sulfonated and therefore negatively charged inner wall, than in column B which was not expected to have fixed charges at the inner wall. There are several possible explanations for the observation of the relatively high EOF in column B. EOF may be generated by the naked silica tubing at the detection window where a 3-mm long section of the PS–DVB inner coating was removed to afford detection. Another explanation is that the formation of a double layer at the neutral inner surface of the capillary either by adsorption of ionic or ionogenic species or by induction of charges at the surface in high electric field.

Fig. 9b illustrates plots of EOF velocity vs. overall electric field strength in the packed columns C and D both having a sulfonated PS–DVB inner surface. Column C was packed with 2-μm fluid impervious, unfunctionalized PS–DVB microspheres and column D with their superficially sulfonated form. As expected higher EOF velocities were obtained with column D than with C due to the strongly negatively charged packing of column D. Finally, Fig. 9c illustrates plots of EOF vs. overall electric field strength as measured with columns having a unfunctionalized inner lining. Column E was packed with the unfunctionalized PS–DVB microspheres whereas the packing in column F consisted of superficially sulfonated PS–DVB particles. It is seen, in agreement with the expectations

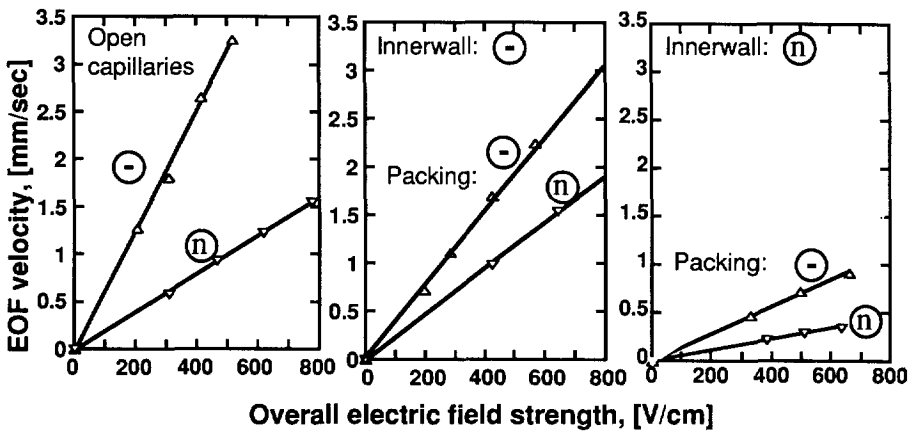

Fig. 9. EOF velocity versus overall electric field strength in fused-silica capillaries having fluid impervious PS–DVB innerlining, either unfunctionalized or sulfonated, and packed with unfunctionalized or sulfonated 2-μm non-porous microspheres. The columns are specified in Table 4. In the graph, the symbols ⊖ refer to negatively charged and ⓝ neutral surfaces respectively. All columns, 26/35 cm×75 μm; eluent, ACN–10 m*M* borate, pH 8.0 (4:1, v/v); tracer, acrylamide; injected for 2 s at 2 kV.

that the EOF was higher with column F than with column E.

In all cases examined so far the EOF generated in the open capillaries having negatively charged inner wall was significantly higher than in any of the packed capillaries even if the zeta potential of the inner wall and the packing could be considered to be about the same. This is exemplified by the 38% decrease in the EOF when column A (open capillary) is packed with sulfonated PS–DVB beads. The EOF generated in column C having a negatively charged inner wall, is higher by 40% when compared to that generated in column F having unfunctionalized wall. The above results illustrate the mutual role of the zeta potential at the capillary inner wall and at the surface of the stationary phase in the generation of EOF. An important finding from these controlled experiments is that upon packing a capillary having fixed charges at the inner surface with a stationary phase, the intensity of the EOF is attenuated as expected from the decreasing electric field strength upon filling the capillary with the packing.

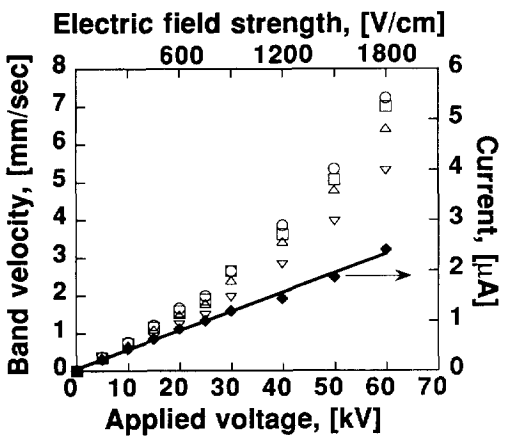

Fig. 10. Plots of the band velocities of acrylamide and three aromatic compounds against the applied voltage up to 60 kV. Column, 23/32 cm×50 μm, raw fused-silica capillary packed with 6-μm Zorbax ODS particles having a mean pore diameter of 300 Å; eluent, ACN–10 m*M* borate, pH 8.0 (4:1, v/v). Sample, (○) acrylamide (□) benzylalcohol (△) benzaldehyde (▽) *o*-dichlorobenzene, injected for 2 s at 2 kV.

4.6. Departure from linearity at high electrical field strength

In order to enhance EOF and to explore CEC at applied voltages higher than 30 kV, the typical upper limit in all commercial CZE units, we used the CEC instrument shown in Fig. 1.

Whereas, the reported EOF velocities obtained by using commercial instruments were generally not higher than 3 mm/s [9,11,17], in our instrument EOF of 6–7 mm/s could be realized at 60 kV with a 23/32 cm×50 μm raw fused-silica capillary packed with 6-μm Zorbax ODS particles as is shown in Fig. 10. The most striking result is that the EOF velocity

is not a linear function of voltage any longer when the field strengths exceed 100 kV/m. A trivial explanation for the non-linearity is that the effect of Joule heating becomes significant and a decrease in viscosity with increasing temperature is responsible for the enhancement of EOF according to Eq. (5). However, the current versus applied voltage plot which is also shown in Fig. 10, is linear up to the highest experimental applied voltage indicating that the cause for the non-linear behavior is something other than Joule heating. It is possible that the non-linearity arises from a polarization of the double layer [42]. This effect has been predicted to come into play when the particles are more conductive than the surrounding electrolyte at high field strengths and results in an EOF significantly higher than that obtained in the conventionally employed domain of the electric field strength. The higher than expected EOF could be advantageous for increasing the speed of separation, even if in analytical applications a linear system observed at lower field strengths generally offers greater reproducibility.

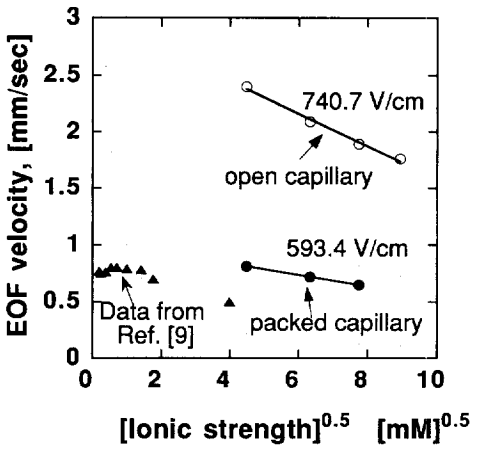

Fig. 11. Effect of salt concentration on EOF in open and packed capillary columns as shown by the plots of EOF velocity against the square root of the added salt concentration. (○) open capillary, 20/27 cm×50 μm; applied voltage, 20 kV (E_T=740.7 V/cm). (●) packed capillary column, 25/34 cm×50 μm, packed with 3.5-μm Zorbax ODS particles having a mean pore diameter of 80 Å; applied voltage, 15 kV (E_T=593.4 V/cm). Eluent, ACN–(10 m*M* Tris–HCl, pH 8.0) (1:1, v/v) and containing 0–60 m*M* NaCl; tracer, acrylamide; injected for 2 s at 2 kV. Data from Knox and Grant [9] are also depicted for comparison.

4.7. Effect of salt concentration

The effect of increasing salt concentration of the mobile phase on EOF velocity is well documented in the literature for open fused-silica capillaries [43–46]. The zeta potential depends on the salt concentration as

$$\xi = \sigma\sqrt{\frac{RT}{2\varepsilon_r\varepsilon_0 cF^2}} \qquad (14)$$

where R is the universal gas constant, T is the absolute temperature, F is the Faraday constant, c is the molar salt concentration and σ the excess charge density. Since, according to Eq. (5) the EOF velocity is directly proportional to ξ, in view of Eq. (14) it will be inversely proportional to the square root of salt concentration.

We measured the effect of increasing salt concentration in both open and packed raw fused capillaries of 50-μm I.D. This was done by adding increasing amounts of NaCl to ACN–10 m*M* Tris–HCl, pH 8.0 (50:50, v/v). As illustrated in Fig. 11, the EOF velocity decreases linearly with the square root of ionic strength in the range from 20–60 m*M* for both open and packed capillaries. The EOF velocity decreases by 35% in the open raw fused-silica capillary and by 39% in the capillary column packed with 3.5-μm ODS particles upon increasing the salt concentration from 0 to 60 m*M*. The data obtained from Knox and Grant [9] is also seen on the graph. At very low Na_2HPO_4 concentrations i.e., from 0.04 to 1 m*M* there is very little change in EOF velocity with increasing salt concentration [47]. However, data from Knox and Grant [9] also shows a decrease of 37% in EOF velocity upon increasing the Na_2HPO_4 concentration from 1 to 10 m*M*.

4.8. Effect of organic modifier concentration

For the effect of increasing organic modifier concentration in CZE it was reported [48] that the EOF decreases with increasing ACN concentration and this was attributed to a concomitant decrease in the zeta potential. We measured the effect of ACN concentration on EOF in open raw fused-silica capillaries in two ways. In one set of experiments the aqueous buffer containing added salt was diluted

serially so that salt concentration decreased upon increasing ACN concentration. In another set of experiments the buffer and salt concentrations were kept constant in the hydroorganic mixtures having various ACN concentrations. The results illustrated in Fig. 12 show that in open raw fused-silica capillaries the EOF velocity decreases with increasing ACN concentration irrespective of whether the salt concentration in the hydroorganic mixture is kept constant or not. Fig. 12 also shows the effect of ACN concentration in 10 m*M* Tris–HCl buffer (pH 8.0) on the EOF velocity in a raw fused-silica capillary packed with 3.5-μm Zorbax ODS particles at constant salt concentration. It is seen in contradistinction to the behavior observed in open capillaries that in the packed capillary the EOF velocity increases with the ACN concentration in the range from 0 to 60%.

The different behavior of ACN concentration on the EOF in open and packed capillaries is striking and falls short of a satisfactory explanation. Similar behavior is reported in the literature [17,49] although other workers [10] observed a 33% decrease in EOF velocity upon increasing ACN concentration from 0 to 60% in CEC columns packed with octadecylated silica. Further investigations are required to elucidate the effect of organic modifiers on the EOF velocity in packed columns for reversed-phase capillary electrochromatography (RPCEC).

4.9. Band spreading in CEC

Perhaps the most important expectation regarding CEC is that the use of electrosmotic flow of the mobile phase results in plate numbers [13] and isocratic peak capacities comparable to those obtained in CZE. Thus, the scope of liquid chromatography could be expanded to facilitate relatively fast separations which require plate numbers higher than 100 000. In Fig. 13 dimensionless van Deemter plots are presented of efficiency data for acrylamide measured with the same column on both micro-HPLC and CEC platforms. Over the velocity range investigated, the reduced plate heights are smaller in CEC than in micro-HPLC mode. Moreover, the Van Deemter curve of the CEC data is flatter at high reduced velocities than the corresponding curve of the micro-HPLC data. The comparison suggests that CEC has a potential for rapid separations and this is supported by the chromatograms of polyaromatic hydrocarbons and aromatic acids shown in Fig. 14.

With our instrument it was possible to apply voltages up to 60 kV and thus obtain an EOF velocity

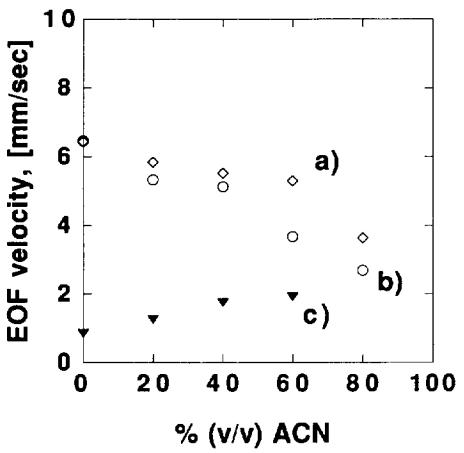

Fig. 12. Effect of ACN concentration on EOF velocity in (a) open capillary at varying salt concentration (b) open capillary at constant salt concentration and (c) packed capillary at constant salt concentration. Open capillary, 20/27 cm×50 μm. Packed capillary, 13/21 cm×50 μm, packed with 3.5-μm Zorbax ODS particles having a mean pore diameter of 80 Å. Eluent, 10 m*M* Tris–HCl (pH 8.0); tracer, acrylamide; injected for 2 kV at 2 s.

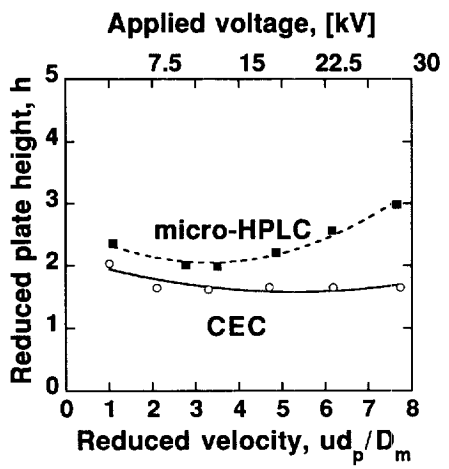

Fig. 13. Plots of reduced plate height against the reduced velocity in a given packed capillary column operated in the CEC and micro-HPLC mode. Column, 23/32 cm×50 μm, raw fused-silica capillary packed with 3.5-μm Zorbax ODS particles having a mean pore diameter of 80 Å; eluent, ACN–10 m*M* borate, pH 8.0 (4:1, v/v); tracer, acrylamide; injected for 2 s at 2 kV.

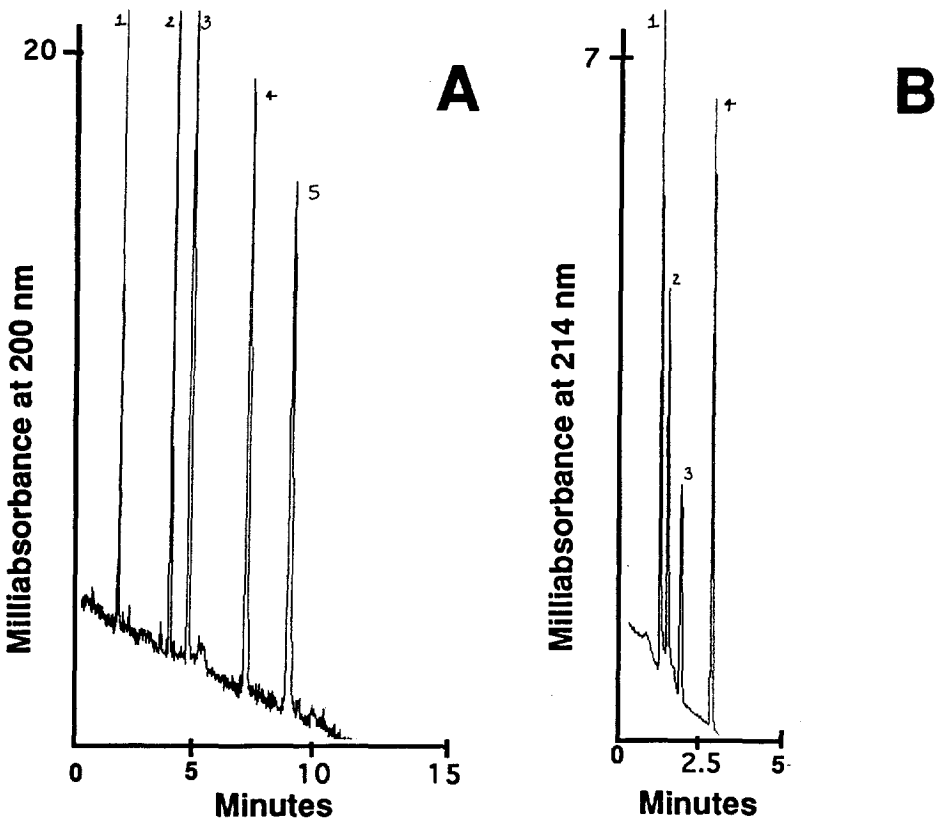

Fig. 14. Electrochromatograms of polyaromatic hydrocarbons and aromatic acids. (A) Sample (1) acrylamide (2) naphthalene (3) fluoranthene (4) biphenyl and (5) *m*-terphenyl; column, 30/39 cm×75 μm, raw fused-silica capillary packed with 3.5-μm Zorbax ODS particles having a mean pore diameter of 80 Å; eluent, ACN–10 m*M* borate, pH 8.0 (4:1, v/v); applied voltage, 30 kV; injection for 2 s at 5 kV. (B) Sample (1) *p*-toluic acid (2) cinnamic acid (3) *p*-terbutyl benzoic acid and (4) *o*-dichlorobenzene; column, 27/36 cm×75 μm, raw fused-silica capillary packed with 6-μm Zorbax ODS particles having mean pore diameter of 80 Å; eluent, ACN–4 m*M* borate, pH 8.5 (4:1, v/v); applied voltage, 30 kV; injection for 2 s at 5 kV.

as high as 6 mm/s to explore band spreading at reduced velocities up to 25. Fig. 15 shows the plot of reduced plate height against the reduced velocity for data measured with small neutral aromatic molecules in RPCEC. The curves exhibit a minima at a reduced velocity of about 5 and then a plateau at h of about 1.6. The rapid separation of small aromatic compounds shown in the electrochromatogram in Fig. 16 demonstrates that the enhanced EOF at high electric field strength is indeed advantageous for fast separations.

Fig. 17 illustrates Van Deemter curves for acrylamide in 180-μm fused-silica capillaries packed with unfunctionalized PS–DVB particles with the mobile phase containing ACN–10 m*M* borate buffer, pH 8.0 (4:1, v/v). Even though the PS–DVB beads were unfunctionalized reduced plate heights in the range of 1.5 to 4 were obtained. The peak shapes for acrylamide were almost Gaussian with an asymmetry factor of 1.004.

It should be noted that in porous stationary phase particles having fixed charges at the pore wall of interconnected and sufficiently wide pores for the double layer not to overlap intraparticular EOF may be generated. This convective mechanism can effectively increase intraparticular mass transfer. As a result, in columns packed with relatively large particles intraparticulate mass transfer resistances could be much smaller in CEC than in classical liquid chromatography where the mass transfer in-

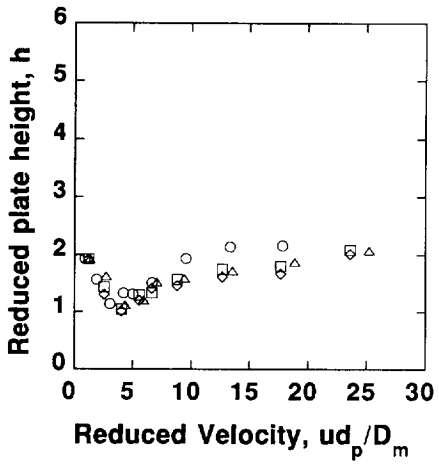

Fig. 15. Reduced Van Deemter plot of RPCEC data obtained with aromatic substances at applied voltages up to 60 kV. Column, 23/32 cm×50 μm, raw fused-silica capillary packed with 6-μm Zorbax ODS particles having a mean pore diameter of 300 Å; eluent, ACN–10 m*M* borate, pH 8.0 (4:1, v/v). Sample, (○) acrylamide, (□) benzylalcohol, (△) benzaldehyde, (▽) *o*-dichlorobenzene; injected for 2 s at 2 kV. The EOF velocity was calculated from the migration velocity of acrylamide. The diffusivities were calculated from Wilke–Chang eq. [52]. The velocity u is the chromatographic velocity of EOF as defined in Eq. (8).

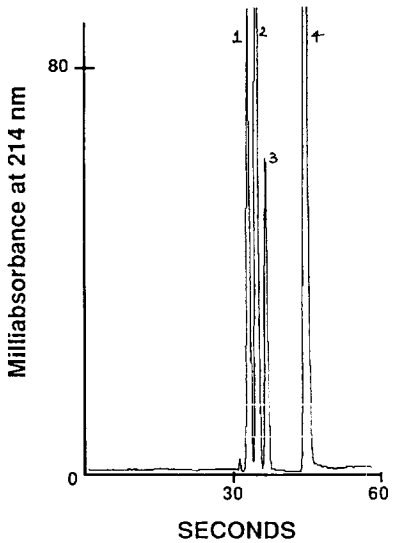

Fig. 16. Chromatogram illustrating the rapid separation of small aromatic compounds at 60 kV applied voltage. Column, 23/32 cm×50 μm, raw fused-silica capillary packed with 6-μm Zorbax ODS particles having a mean pore diameter of 300 Å; eluent, ACN–10 m*M* borate, pH 8.0 (4:1, v/v). Sample, (○) acrylamide, (□) benzylalcohol, (△) benzaldehyde, (▽) *o*-dichlorobenzene; injected for 2 s at 2 kV.

side the particles occurs solely by diffusion. This resembles the enhancement of intraparticle mass transfer by a convective mechanism observed in gigaporous column packings in the liquid chromatography of slowly diffusing species [50]. Fig. 18 illustrates isocratic separation of peptides on an 8-μm 1000 Å polymeric strong cation exchanger with ACN–25 m*M* phosphate, pH 3.5 (2:3, v/v). Reduced plate heights of 1.1 or lower were obtained for most sample component.

4.10. Comparison of column lengths in micro-HPLC and CEC

In micro-HPLC, the maximum permissible column length at a given pressure drop and chromatographic flow velocity can be related to the diameter of the packing as

$$L = \frac{\Delta P}{\eta u_c} \frac{d_p^2 \varepsilon_e^3}{180(1-\varepsilon_e)^2 \varepsilon_T} \qquad (15)$$

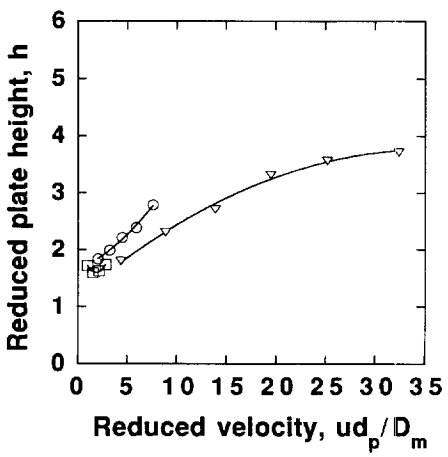

Fig. 17. Plots of the reduced plate height against reduced velocity measured in raw fused-silica capillary columns packed with spherical gigaporous (1000 Å) PLRP particles of (□) 5-μm (◇) 8-μm and (▽) 20-μm diameter. Column, 30/40 cm×180 μm, raw fused-silica capillary; eluent, ACN–10 m*M* borate, pH 8.0 (4:1, v/v); tracer, acrylamide; injected for 2 s at 2 kV. For the velocity frame used see Fig. 15.

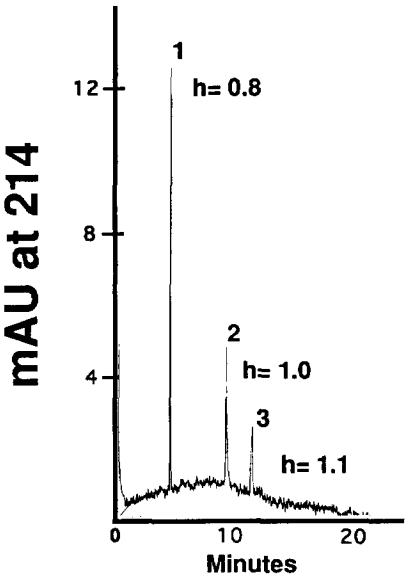

Fig. 18. Electrochromatogram of peptides obtained with a strong cation exchanger column. Column, 28/37 cm×180 μm, raw fused-silica capillary packed with 8-μm gigaporous (1000 Å) PLSCX strong cation exchanger; eluent, ACN–25 m*M* phosphate, pH 3.5 (2:3, v/v); applied voltage, 15 kV. Sample, (1) acrylamide, (2) Trp–Gly–Gly–Phe–Met, (3) Trp–Met–Asp–Phe; injected for 2 s at 2 kV.

For a η value of 0.5 cp, which is reasonable for a mobile phase containing 80% acetonitrile and ε_T, ε_e values of 0.6 and 0.4 respectively, the maximum permissible column length, L, to attain a velocity of 3 mm/s at 300 bar pressure drop was calculated according to Eq. (15) as a function of the particle diameter, d_p and the results are illustrated in Fig. 19.

For CEC, the electrokinetic permeability can be obtained from Fig. 5 as the slope of linear flow velocity versus overall electric field strength plot. The values of electrokinetic permeability for 3.5-μm and 6-μm porous particles and 2-μm non-porous particles are 3.3, 3.9 and $4.6 \cdot 10^{-4}$ cm^2/s V, respectively for ACN–10 m*M* borate buffer, pH 8.0 (4:1, v/v). These values were used to calculate the maximum permissible column length for each particle diameter for a linear flow velocity of 3 mm/s at a voltage drop of 30 kV. For the non-porous 2-μm particles the EOF velocity was reduced by a factor of 1.5 so that for sake of consistency, the EOF was corrected to the chromatographic electrosmotic velocity.

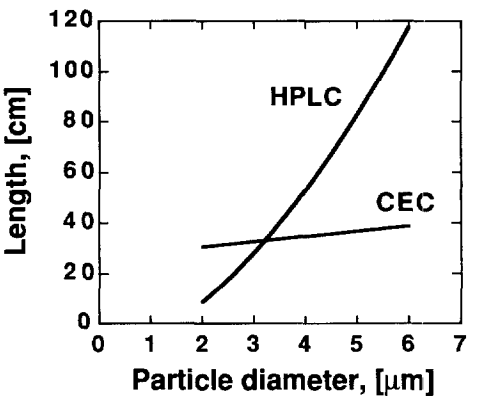

Fig. 19. Plots illustrating of the maximal column length as a function of particle diameter in CEC and HPLC. The respective maximum applied voltage and the maximum permissible column inlet pressure were taken as 30 kV and 300 bar in CEC and HPLC, with the eluent velocity fixed at 3 mm/s. The conditions for the CEC data were the same as in Fig. 4.

The results are plotted in Fig. 19 to show that, whereas the maximum permissible column length is a strong function of the particle diameter in micro-HPLC, it is a rather weak function in CEC. Thus, CEC facilitates the use of relatively long columns packed with small particles that could not be employed in micro-HPLC because the required pressure drop would be prohibitively high. In HPLC most separations are carried out by using less than 10 000 theoretical plates. Under such conditions the peak capacity is insufficient for the separation of samples having a large number of components even if the peak capacity can be enhanced by gradient elution [51]. Thus, the high plate efficiency of CEC, upon exploiting its full potential, may offer new avenues for the separation of multicomponent mixtures by liquid chromatography. Fig. 20 illustrates the separation of polyaromatic hydrocarbons compounds on a 30-cm long (A) a 50-cm long (B) column. The EOF velocities and reduced plate heights were about the same for both columns.

5. Conclusions

The results of this study lend support to the general expectation that a major advantage of CEC rests with the possibility of readily attaining rela-

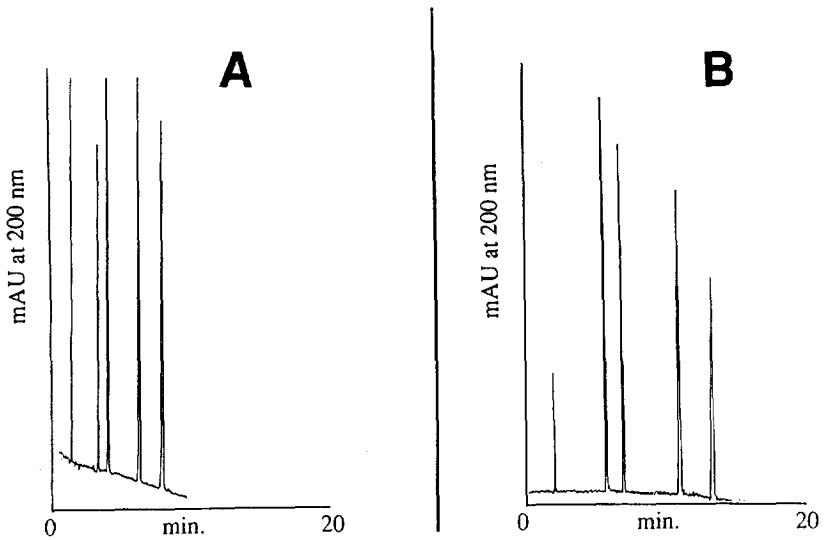

Fig. 20. Effect of column length in CEC as illustrated by the separation of polyaromatic hydrocarbons on a 40-cm (A) and a 50-cm long (B) column. In both cases 50 μm i.d. capillary was packed with 3.5-μm Zorbax ODS particles having a mean pore diameter of 80 Å; eluent, ACN–10 m*M* borate, pH 8.0 (4:1, v/v); applied voltage, 10 kV (A) and 50 kV (B). Sample, (1) acrylamide, (2) naphthalene, (3) fluoranthene, (4) biphenyl, (5) *m*-terphenyl; injected for 2 s at 5 kV.

tively high flow-rates in capillary columns packed with small particles that would require prohibitively high column inlet pressures in HPLC due to their low permeability. However, further theoretical and experimental studies are needed to gain insight into the effect of packing structure on the current and the EOF on the scale of the capillary and the particle diameter.

The column in CEC is unique as it consists of a packed and an open segment having different conductances. This can be the source of several inherent problems associated with the measurement of EOF velocity in CEC. It is not surprising therefore that the data presently available on the generation, magnitude and control of EOF is rather scarce and falls short of being sufficiently accurate to serve as a basis for a detailed understanding of EOF in porous media.

It is eminently clear that a great deal of investigations are needed to explicate the physicochemical phenomena underlying the separation process in CEC besides a better understanding of the nature of EOF in packed columns. A quantum jump in the stationary phase design is required to develop new column packings suitable for the separation of various types of samples, e.g., proteins and complex carbohydrates with high speed and efficiency. Lastly, novel ways for high resolution separations of practical interest should be found within the broad concept of CEC.

Acknowledgements

This work was supported by Grant No. GM 20993 from the National Institute of Health, US Public Health Service. The advise by Norman Smith was very helpful in the initial design of our CEC unit. The assistance by Peter Kindlmann, of the Faculty of Engineering, Yale University in designing and Glenn Whitehouse, of Analytica of Branford in implementing the high voltage power supply assembly is appreciated. We wish to thank Dr. Frank Warner and Dr. Jack Kirkland for the gift of stationary phases. Our particular thanks are due to Dr. Xian Huang for preparing PS–DVB microspheres and capillaries with PS–DVB innerlining.

References

[1] M. von Smoluchowski, in L. Graetz (Editor), Handbuch der Electrizität und des Magnetism, Vol. 2, Verlag von Johann Ambrosius Barth, Leipzig, 1921, pp. 366.
[2] D.L. Mould, R.L.M. Synge, Analyst 77 (1952) 964.
[3] D.L. Mould, R.M.L. Synge, Biochem. J. 58 (1954) 571.
[4] V. Pretorius, B.J. Hopkins, J.D. Schieke, J. Chromatogr. 99 (1974) 23.
[5] J.W. Jorgenson, K.D. Lukacs, J. Chromatogr. 218 (1981) 209.
[6] T. Tsuda, Anal. Chem. 59 (1987) 521.
[7] T. Tsuda, Anal. Chem. 60 (1988) 1677.
[8] J.H. Knox, I.H. Grant, Chromatographia 24 (1987) 4017.
[9] J.H. Knox, I.H. Grant, Chromatographia 32 (1991) 317.
[10] H. Yamamoto, J. Baumann, F. Erni, J. Chromatogr. 593 (1992) 313.
[11] C. Yan, D. Schaufelberger, F. Erni, J. Chromatogr. A 670 (1994) 15.
[12] N.W. Smith, M.B. Evans, Chromatographia 38 (1994) 649.
[13] N.W. Smith, M.B. Evans, Chromatographia 41 (1995) 197.
[14] R.J. Boughtflower, T. Underwood, C.J. Paterson, Chromatographia 40 (1995) 329.
[15] B. Behnke, E. Bayer, J. Chromatogr. A 680 (1994) 93.
[16] C. Yan, R. Dadoo, R.N. Zare, D.J. Rakestraw, D.S. Anex, Anal. Chem. 68 (1996) 2726.
[17] M.M. Dittmann, G.P. Rozing, J. Chromatogr. A 744 (1996) 63.
[18] L.J. Klinkenberg, Am. Petrol. Inst. Drilling Prod. Pract. (1941) 200.
[19] H. Engelhardt, W. Beck, T. Schmitt, Capillary Electrophoresis: Methods and Potential, Vieweg, Wiesbaden, 1996, p. 9
[20] G.M. Janini, H.J. Issaq, in N.A. Guzman (Editor), Capillary Electrophoresis Technology, Marcel Dekker, New York, 1993, p. 124.
[21] J. Bear, Dynamics of fluids in porous media, Dover Publications, New York, 1988, p. 111.
[22] J.R. Boyack, J.C. Giddings, Arch. Biochem. Biophys. 100 (1963) 16.
[23] J.T. Edward, Adv. Chromatogr. 2 (1966) 63.
[24] M. Tassopoulos, D.E. Rosner, Chem. Eng. Sci 42 (1991) 421.
[25] G.E. Archie, Trans. A.I.M.E. 146 (1941) 54.
[26] R.E. de la Rue, C.W. Tobias, J. Electrochem. Soc. 106 (1959) 827.
[27] M. von Smoluchowski, Bull. Int. Acad. Sci. Cracovie 1 (1903) 184.
[28] S.F.Y. Li, Capillary Electrophoresis: Principles, Practice and Applications, Elsevier, Amsterdam, 1992, p. 201.
[29] C.L. Rice, R. Whitehead, J. Phys. Chem. 69 (1965) 4017.
[30] T. Tsuda, K. Nomura, G. Nakagawa, J. Chromatogr. 248 (1982) 241.
[31] Q. Wan, Anal. Chem. 69 (1997) 361.
[32] A.E. Scheidegger, Petrol. Eng. 25 (1953) B121.
[33] Cs. Horváth, H.J. Lin, J. Chromatogr. 126 (1976) 401.
[34] Cs. Horváth and W.R. Melander, in E. Heftmann (Editor), Chromatography, Elsevier, Amsterdam, 1983, pp. A93–A94.
[35] X. Huang, Cs. Horváth, J. Chromatogr. A, in press.
[36] R.J. Boughtflower, T. Underwood, J. Maddin, Chromatographia 41 (1995) 398.
[37] R.W. O'Brien, W.T. Perrins, J. Colloid Interface Sci. 99 (1984) 20.
[38] J.C. Sternberg, R.E. Poulson, Anal. Chem. 36 (1964) 1492.
[39] H. Halasz, I. Heine, Nature 194 (1962) 971.
[40] L. Várady, K. Kalghatgi, Cs. Horváth, J. Chromatogr. 458 (1988) 207.
[41] K. Kalghatgi, Cs. Horváth, J. Chromatogr. 398 (1987) 335.
[42] S.S. Dukhin, Adv. Colloid Interface Sci. 35 (1991) 173.
[43] K.D. Altria, C.F. Simpson, Anal. Proc. 25 (1988) 85.
[44] K.D. Altria, C.F. Simpson, Chromatographia 24 (1987) 527.
[45] W. Nashabeh, Z. El Rassi, J. Chromatogr. 514 (1990) 57.
[46] G.J.M. Bruin, J.P. Chang, R.H. Kuhlman, K. Zegers, J.C. Kraak, H. Poppe, J. Chromatogr. 471 (1987) 429.
[47] S.E. van den Bosch, S. Heemstra, J.C. Kraak, H. Poppe, J. Chromatogr. A 755 (1996) 165.
[48] C. Schwer, E. Kenndler, Anal. Chem. 63 (1991) 1801.
[49] H. Rebscher, U. Pyell, Chromatographia 38 (1994) 737.
[50] D. Frey, E. Schweinheim, Cs. Horváth, Biotechnol. Prog. 9 (1993) 273.
[51] Cs. Horváth, S.R. Lipsky, Anal. Chem. 39 (1967) 1893.
[52] R.C. Ried, J.M. Prausnitz, B.E. Poling, The Properties of Gases and Liquids, McGraw–Hill, New York, 1987, p. 598.